Characterization of bimetallic surface structures of highly active Rh–Sn/SiO_2 catalysts for NO–H_2 reaction by EXAFS

Keiichi Tomishige, Kiyotaka Asakura and Yasuhiro Iwasawa[1]

Department of Chemistry, Faculty of Science, The University of Tokyo, Hongo, Bunkyo-ku, Tokyo 113, Japan

Rh–Sn/SiO_2 catalysts prepared by the reaction of $(CH_3)_4Sn$ with Rh metal particles supported on SiO_2 have remarkably high activities for NO–H_2 reaction and NO dissociation. The bimetallic surface structure of Rh–Sn/SiO_2 composed of an isolated Rh atom surrounded by six Sn atoms, is presented by Rh K-edge and Sn K-edge EXAFS, FT-IR, TEM and CO adsorption.

Keywords: EXAFS; Rh–Sn/SiO_2; NO–H_2 reaction; NO dissociation; bimetallic ensemble structure

1. Introduction

Bimetallic catalysts containing Sn have been demonstrated to be active for CO oxidation and ethyl acetate hydrogenation [1–5] because of the preferable interaction of Sn with oxygen atom. The bimetallic catalysts prepared by the reaction between alkyl tin and oxide-supported metal particles show different activity from the catalysts prepared by a coimpregnation method [2–7]. We have found that Rh–Sn/SiO_2 catalysts which are prepared by the selective reaction of $(CH_3)_4Sn$ and Rh/SiO_2 have much higher activity than Rh/SiO_2 and coimpregnation Rh–Sn/SiO_2 for NO dissociation and NO–H_2 reaction [6]. On Rh–Sn/SiO_2, NO molecules are nearly instantaneously decomposed at room temperature, while NO molecularly adsorbs on Rh/SiO_2 and does not decompose significantly below 373 K. The catalytic activity (steady-state reaction rate) of Rh–Sn/SiO_2 for the NO–H_2 reaction increases with an increase of Sn added in the range of Sn/Rh $\leqslant 0.4$, showing an S-shape dependency. At Sn/Rh = 0.4 the activity becomes highest and the turnover frequency (TOF) at 373 K is 75 times as high as that of Rh/SiO_2. In NO–H_2 reaction on Rh/SiO_2, the rate-determining step has been reported to be NO dissociation assisted by an adsorbed H atom [8]. It was suggested that the

[1] To whom correspondence should be addressed.

$NO–H_2$ reaction on $Rh–Sn/SiO_2$ proceeds by a different reaction mechanism involving the reaction of H_2 with SnO_x produced during NO dissociation [6]. In this report, the bimetallic surface structures of $Rh–Sn/SiO_2$ after reduction and during $NO–H_2$ reaction were characterized by EXAFS (mainly), FT-IR, TEM, and CO adsorption, to find essential factors for the genesis of promoter effects.

2. Experimental

SiO_2 was immersed with a methanol solution of $RhCl_3 \cdot 3H_2O$, followed by drying at 393 K for 12 h and reduction with H_2 at 573 K. The Rh particles on SiO_2 were reacted with $(CH_3)_4Sn$ vapor at 423 K, at which temperature no $(CH_3)_4Sn$ reacted with the SiO_2 support. The catalysts were reduced with H_2 at 573 K for 1 h, followed by evacuation before each run. The loading of Rh was always 1.0 wt% and the Sn/Rh ratio was varied in the range 0–1. Coimpregnation $Rh–Sn/SiO_2$ catalysts (denoted as Imp-$Rh–Sn/SiO_2$) were prepared from a methanol solution of $RhCl_3 \cdot 3H_2O$ and $SnCl_2$. Residual chlorides were not observed or were negligible by XPS. NO dissociation and $NO–H_2$ reaction were carried out in the temperature range 273–393 K in a closed circulating system (volume: 200 cm^3), producing N_2O and N_2, which were analyzed by gas chromatography.

X-ray absorption spectra at the Rh K-edge and Sn K-edge spectra were measured at the EXAFS facilities installed at the BL-10B and BL-6B in the National Laboratory for High Energy Physics, respectively (Proposal No. 90-003) with a positron energy of 2.5 GeV and a storage ring current of 250–350 mA. EXAFS data were collected in a transmission mode using ionization chambers filled with Ar for the I_0 signal and Kr for the I signal. The samples were treated in situ in a closed circulating system and transferred to an EXAFS glass cell with thin glass windows without contacting air. The EXAFS spectra were measured at room temperature or 70 K. The phase shift and amplitude function for Rh K-edge EXAFS was empirically extracted from Rh foil. The curve-fitting analysis on Sn K-edge EXAFS was carried out with the theoretical phase shift parameter (absorbing atom Sn and scattering atom Rh) [9] and empirical amplitude function extracted from Rh foil measured at 70 K. The reason we used these parameters is that it was difficult to distinguish between Rh and Sn as backscattering atoms.

3. Results

Fig. 1 shows the Fourier transforms of Sn K-edge EXAFS spectra for $Rh–Sn/SiO_2$ after H_2 reduction. The peak at 0.2–0.3 nm is attributed to Sn–Rh or Sn–Sn bonding. Tin–oxygen bonds which should appear at 0.1–0.2 nm were not observed, indicating that little or no Sn is present as oxides on SiO_2. According to the curve-fitting analysis, the bond length of Sn–Rh or Sn–Sn was determined to be 0.270 nm which is much smaller than the bond distance of α-Sn (0.282 nm) and β-Sn

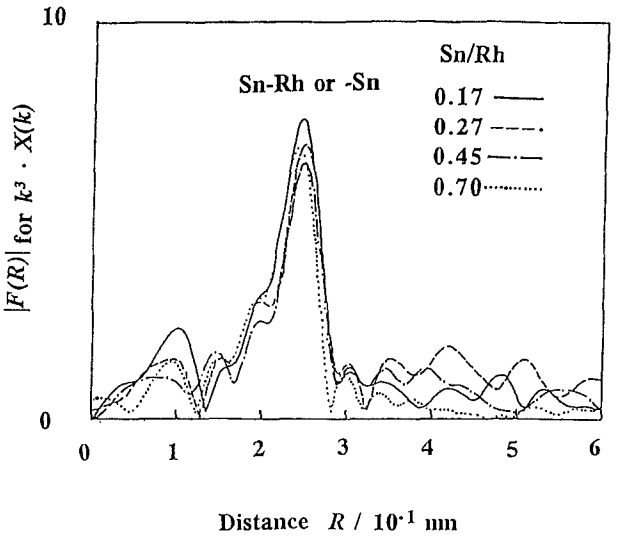

Fig. 1. Fourier transforms of Sn K-edge EXAFS spectra on Rh–Sn/SiO_2; measurement temperature: 298 K, Fourier transform range: 30–120 nm^{-1}.

(0.302 nm) and similar to that of Rh metal itself. These findings suggest that all Sn atoms intrude into the Rh metal lattice to form Rh–Sn alloy [10,11].

Fig. 2 shows the Fourier transforms of Sn K-edge EXAFS spectra for Rh–Sn/SiO_2 (Sn/Rh = 0.3 and 0.7) and the Imp-Rh–Sn/SiO_2 (Sn/Rh = 0.3) after reduction with H_2 at 573 K and after oxidation with O_2 at 298 K. When Rh–Sn/SiO_2 (Sn/Rh = 0.3) was oxidized at 298 K, Sn–O bonds appeared, while Sn–Rh or Sn–Sn bonding disappeared almost completely. This suggests that all Sn atoms are located at the surface to be oxidized. At Sn/Rh = 0.7, a part of Sn–Rh or Sn–Sn bonds remained, indicating that all the Sn atoms were not readily accessible to oxygen. Therefore, the Rh–Sn bimetallic phase is also present below the surface of particles for Sn/Rh = 0.7. In contrast to Rh–Sn/SiO_2 catalysts prepared by the selective reaction of $(CH_3)_4Sn$ and Rh particles on SiO_2, on the Imp-Rh–Sn/SiO_2 even at Sn/Rh = 0.3 a part of the Sn atoms were not oxidized, indicating that a large number of Sn atoms are present inside the particles.

Fig. 3 shows the Fourier transforms for Rh K-edge EXAFS spectra of Rh–Sn/SiO_2, and the coordination numbers and Debye–Waller factors by curve-fitting analysis. The intensity of the peak which is attributed to Rh–Rh bonding decreased gradually by the addition of Sn. The coordination number of the Rh–Rh bond decreased linearly by the addition of Sn. The decrease in coordination number is not due to the decrease of the particle size, because the metal particle sizes of Rh/SiO_2 and Rh–Sn/SiO_2 (Sn/Rh = 0.45) are almost the same (2.5 ± 0.3 nm) by TEM observation. Debye–Waller factors were constant in the range of Sn/Rh $\leqslant$ 0.3, and increased at Sn/Rh = 0.38. The Debye–Waller factor became constant again at Sn/Rh $\geqslant$ 0.4.

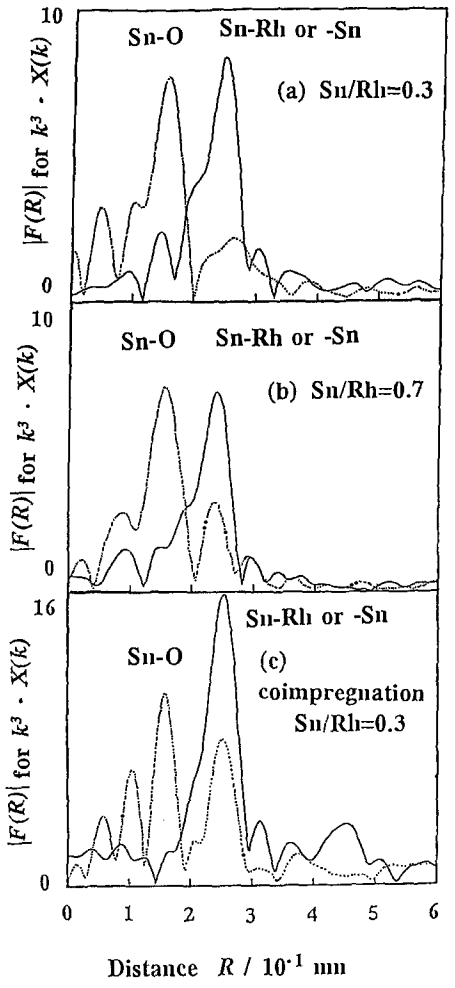

Fig. 2. Fourier transforms of Sn K-edge EXAFS spectra for Rh–Sn/SiO_2 before (solid line) and after (dotted line) oxidation with O_2 at 298 K; measurement temperature: (a) 70 K; (b), (c) 298 K, Fourier transform range: 30–120 nm^{-1}

Fig. 4 shows the Fourier transforms of Sn K-edge EXAFS for Rh–Sn/SiO_2 (Sn/Rh = 0.45) under different conditions (reduction, NO exposure at 373 K and NO–H_2 reaction at 373 K). The Sn–O bonds appeared with the sample exposed to NO or during NO–H_2 reaction, while Sn–Rh or Sn–Sn bonding retained almost completely.

4. Discussion

From the Sn K-edge EXAFS spectra for the Imp-Rh–Sn/SiO_2 (Sn/Rh = 0.3) in fig. 2c, the peak intensity of Sn–Rh or Sn–Sn bonds decreased to about half of the

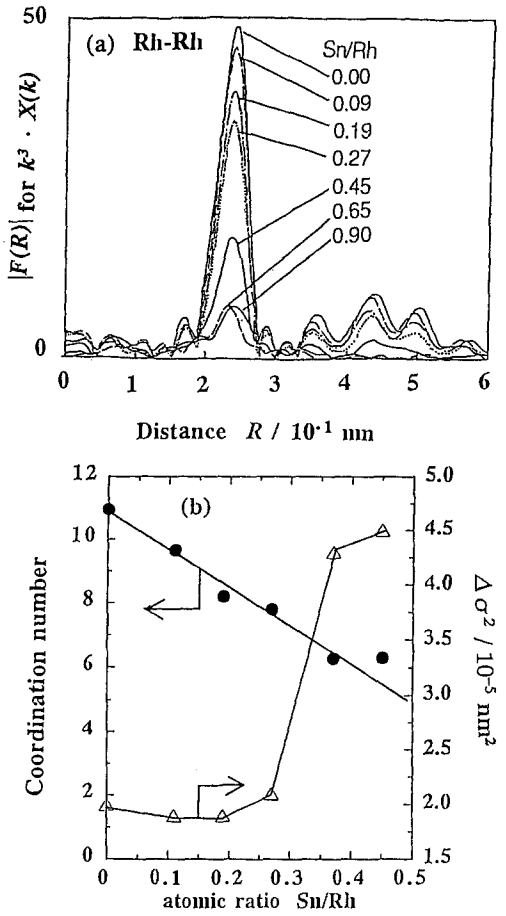

Fig. 3. (a) Fourier transforms of Rh K-edge EXAFS spectra and (b) coordination numbers of Rh–Rh bond and Debye–Waller factors by curve-fitting analysis; measurement temperature: 298 K, Fourier transform range: 30–150 nm^{-1}.

original intensity by oxidation at 298 K, suggesting that about half of Sn atoms in the Rh–Sn bimetallic catalyst prepared by the coimpregnation method are located inside the metal particles even at Sn/Rh = 0.3. In contrast, for the Rh–Sn/SiO_2 prepared by the selective bimetallic reaction of $(CH_3)_4Sn$ with Rh metal particles supported on SiO_2, Sn atoms of the bimetallic particles at Sn/Rh $\leqslant$ 0.4 are all accessible to oxygen to form Sn–O bonds at 298 K as typically shown in fig. 2a for the sample of Sn/Rh = 0.3. The catalysts with Sn/Rh = 0.7 showed the formation of Sn–O bonds by exposure to O_2 at 298 K in fig. 2b, indicating intrusion of an excess of Sn atoms more than Sn/Rh = 0.4 into the Rh particles (probably to the second layer). The amount of CO adsorption on Rh–Sn/SiO_2 decreased linearly with increasing Sn quantity in the range of Sn/Rh $\leqslant$ 0.38, and was constant in the range of Sn/Rh $\geqslant$ 0.4 [6]. This well coincides with the EXAFS analysis.

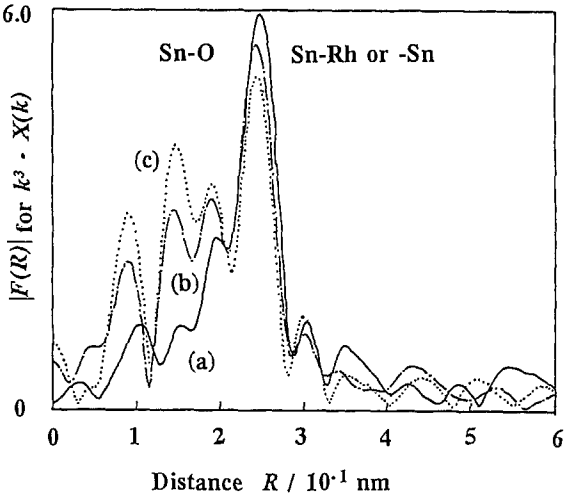

Fig. 4. Fourier transforms of Sn K-edge EXAFS spectra for Rh–Sn/SiO_2 (Sn/Rh = 0.45): (a) after H_2 reduction at 573 K (solid line); (b) in the steady state NO–H_2 reaction at 373 K (broken line); (c) after NO exposure at 373 K (dotted line); measurement temperature: 298 K, Fourier transform range: 30–120 nm^{-1}.

There are two possibilities for the location of Sn atoms; adsorption on the Rh particle surface and bimetallic surface layer at the particle surface. Little change in the peak intensity of Sn–Rh or Sn–Sn in the Fourier transform of Sn K-edge EXAFS with the Sn content implies the incorporation of Sn to the first layer of Rh particle surface rather than the adsorption on Rh particles (Sn/Rh $\leqslant$ 0.4) followed by the incorporation into the particles (Sn/Rh $\geqslant$ 0.4). The large decrease in the coordination number of the Rh–Rh bond in fig. 3 also supports this model, because if Sn atoms merely adsorb on the Rh particles, the coordination number would not decrease [12]. The discontinuous increase of the Debye–Waller factor at Sn/Rh = 0.4 in fig. 3 may be ascribed to a large distortion at the bimetallic monolayer with Sn/Rh = 0.4 by the difference in the intrinsic atomic radius between Sn and Rh. The Sn–Rh bond of 0.270 nm is shorter than the sum (0.275 nm) of Rh radius and Sn radius. The formation of the bimetallic monolayer at Sn/Rh = 0.4 is expected to increase the metal particle size from 2.5 nm to 2.8 nm on average. Then we can estimate the surface composition for the catalyst of Sn/Rh = 0.4 by CO adsorption experiments to be Sn : Rh = 3 : 1. Fig. 5 illustrates a surface model for the Rh–Sn bimetallic catalyst prepared by the reaction of $(CH_3)_4Sn$ and Rh metallic particles followed by H_2 reduction at 573 K, where the fcc(1 1 1) plane is assumed to be exposed as the most stable plane[#1]. Only linear CO was observed with Rh–Sn/SiO_2 (Sn/Rh = 0.4) [12], which coincides with this structure for a Rh atom being surrounded by six Sn atoms to be isolated (fig. 5). The catalytic activity

[#1] The more detailed surface ensemble structure will be discussed in a following paper [12].

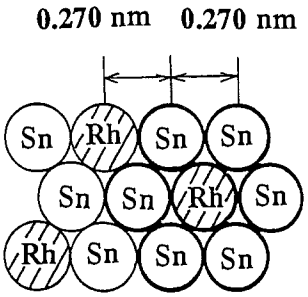

Fig. 5. A model surface structure of Rh–Sn/SiO_2 (Sn/Rh= 0.4).

(TOF) of Rh–Sn/SiO_2 for NO–H_2 reaction increased with an S-shape dependency by the addition of Sn and saturated at Sn/Rh = 0.4. This profile also coincides with the above Rh–Sn ensemble structure as active sites. Fig. 4 shows the formation of Sn–O bonds by NO dissociation, while Sn–Rh or Sn–Sn bonds are retained. As a result, the promoting effect of Sn on Rh catalysis is ascribed to the Rh–Sn bimetallic ensemble sites efficiently created by the selective reaction of $(CH_3)_4Sn$ with Rh metal particles on SiO_2, which exhibit high catalytic activity for NO reduction with H_2 due to a remarkably high activity for NO dissociation [6]. The bond distance of Sn–O in produced SnO_x was 0.205 nm by the EXAFS analysis. The slowest step in the catalytic NO–H_2 reaction is likely the reduction of the SnO_x with H_2, showing a balance of the SnO_x formation by NO dissociation and its reduction in the steady state of reaction as shown in fig. 4b [6,12].

It is to be noted that the Rh–Sn bimetallic ensemble sites having an isolated Rh atom surrounded by Sn atoms, which exhibit remarkably high activity for NO dissociation and NO–H_2 reaction, can be produced in an atomic scale by the selective bimetallic reaction of $(CH_3)_4Sn$ with Rh particles on SiO_2, followed by reduction with H_2, as characterized by careful EXAFS analyses.

References

[1] M. Masai, K. Nakahara and M. Yabashi, Chem. Lett. (1979) 502.
[2] D. Didillon, A. El Mansour, J.P. Candy, J.M. Basset, F. Le Peltier and J.P. Bournonville, in: *Preparation of Catalysts V*, Studies in Surface Science and Catalysis, Vol. 63, eds. G. Poncelet, P.A. Jacobs, P. Grange and B. Delmon (Elsevier, Amsterdam, 1991) p. 717.
[3] J.P. Candy, A. El Mansour, O.A. Ferretti, G. Mabilon, J.P. Bournonville, J.M. Basset and G. Martino, J. Catal. 112 (1988) 201.
[4] J.P. Candy, O.A. Ferretti, G. Mabilon, J.P. Bournonville, A. El Mansour, J.M. Basset and G. Martino, J. Catal. 112 (1988) 210.
[5] M. Agnelli, J.P. Candy, J.M. Basset, J.P. Bournonville and O.A. Ferretti, J. Catal. 121 (1990) 236.
[6] K. Tomishige, K. Asakura and Y. Iwasawa, J. Chem. Soc. Chem. Commun., in press.
[7] J.L. Margitfalvi, H.P. Jalett, E. Talas, A. Baiker and H.U. Blaser, Catal. Lett. 10 (1991) 325.

[8] W.C. Hecker and A.T. Bell, J. Catal 88 (1984) 289.
[9] B.K. Teo and P.A. Lee, J. Am. Chem. Soc. 101 (1979) 2815.
[10] R.L. Cohen, L.C. Feldman, K.W. West and B.M. Kincaid, Phys. Rev. Lett. 49 (1982) 1416.
[11] S.H. Overbury and Y. Ku, Phys. Rev. B 46 (1992) 7868.
[12] K. Tomishige, K. Asakura and Y. Iwasawa, to be published.